J. Fluid Mech. (1994), vol. 272, pp. 235–254

On the instability of wave-catalysed longitudinal vortices in strong shear

By W.R.C. PHILLIPS AND Z. WU

Department of Mechanical and Aeronautical Engineering,
Box 5725, Clarkson University, Potsdam, NY 13699-5725, USA

(Received 7 July 1993 and in revised form 21 February 1994)

The inviscid instability of $O(\epsilon)$ two-dimensional periodic flows to spanwise-periodic longitudinal vortex modes in parallel $O(1)$ shear flows is considered. In such cases, not only is the effect of fluctuations upon the mean state important but also the influence of the developing mean flow on the fluctuating part of the motion. The former is described by a generalized Lagrangian-mean formulation; the latter by a modified Rayleigh equation. Of specific interest is whether the spanwise distortion of the wave field feeds back to enhance or inhibit instability to longitudinal vortex form. Two cases are considered in detail: uniform shear between wavy walls and non-uniform shear beneath free-surface waves. In both cases wave distortion acts to inhibit, and in some circumstances curtail, instability for all but the shortest waves.

1. Introduction

Longitudinal vortices are widely observed in fluid flow situations that exhibit both mean and fluctuating parts. As Langmuir circulations near the wind-driven surface of open bodies of water they act to mix nutrients and other biological material (Leibovich 1983); in the wall region of turbulent boundary layers they are closely linked to the regeneration of turbulence (Robinson 1991); while in the wake of surface marine vessels their presence and persistence give rise to footprints that last for hours, sometimes days (Sarpkaya & Henderson 1984).

Initial attempts to explain the genesis of such vortices do so in the context of unstable laminar boundary layers where they form, in concert with oblique wave modes, from initially small spanwise disturbances. Such observations led Benney & Lin (1960), Benney (1964) and others to consider the interaction of selected two-dimensional and oblique wave modes. But this model postulates rather than explains the existence of a strongly y-periodic wave field (Craik 1985) and although longitudinal vortices can arise in such circumstances, they first grow only algebraically in time t. Another possibility is that the two-dimensional periodic flow is itself unstable to disturbances of longitudinal vortex form; nonlinear coupling between the two-dimensional waves and the spanwise periodic flow may then generate oblique wave modes (Herbert & Morkovin 1980). In this instance the vortices grow exponentially with time, at least until a finite-amplitude equilibrium is reached. An example is the Craik–Leibovich type 2 (CL2) instability (Craik 1977; Leibovich 1977, 1983), conceived as an explanation for Langmuir circulations; a second example is discussed by Phillips (1993).

Essential for CL2 to occur is the presence of a wavy disturbance having a sheared pseudomomentum, together with pre-existing vorticity imparting an Eulerian-mean

shear in the same sense as the pseudomomentum. When the pre-existing vorticity is weak ($O(\epsilon^2)$ or smaller), the pseudomomentum is equivalent to the Stokes drift and a kinematic description of (an inviscid flow subject to) the instability is possible: namely that the Stokes drift gradient causes vortex lines (which move with the fluid) to tilt streamwise wherever the Eulerian-mean shear is laterally distorted, giving rise to a longitudinal component of vorticity and ultimately vortices.

But the mechanism is not wave driven (McIntyre & Norton 1990); rather waves act, through the pseudomomentum, as a catalyst. In consequence the magnitude of the mean flow change is not uniformly bound, in the case of $O(\epsilon)$ waves, by $O(\epsilon^2)$, but is likely to be governed by the magnitude of the pre-existing vorticity in the initial state.

As the magnitude of the mean flow change increases, however, so too does the degree to which it modifies the wave field; thus, might it distort the waves enough to destroy their catalytic action at some stage, or does it enhance the instability? Indeed 'the ultimate fate of an inviscid flow subject to the instability.., and in which the initial vorticity is arbitrarily strong, ..is still an open question' (McIntyre & Norton). Of course the barrier to progress is in explicitly calculating the back effect of the mean flow modification upon the wave field. Craik (1977), Leibovich (1977, 1980, 1983) and Leibovich & Paolucci (1981) restrict attention to examples with negligible wave distortion, i.e. to vorticity fields of $O(\epsilon)$ or smaller; only Craik (1982*b*) considers CL2 in strong shear†. Craik posed the appropriate eigenvalue problem for inviscid $O(1)$ vorticity fields and realized that definite results could be obtained analytically when the spanwise spacing of the vortices is small. But although he was able to demonstrate the existence of longitudinal vortex instability in this limit, he did not ascertain whether wave distortion acted to enhance or inhibit the instability. Our purpose is to resolve that question numerically and in the process remove any restriction on the spanwise spacing of the vortices.

In constructing the eigenvalue problem for strong Eulerian-mean shear in the presence of two-dimensional rotational wavy disturbances, Craik (1982*a*,*b*), referred to hereafter as C*a* and C*b* respectively, assumes $O(\epsilon)$ waves and employs Andrews & McIntyre's (1978) generalized Lagrangian-mean (GLM) equations. GLM (see § 2.1) describes only the effect of fluctuations upon the mean state, however, and so a further equation is necessary to account for the influence of the developing mean state upon the fluctuating part of the motion; we refer to that equation as the Rayleigh–Craik equation (§ 2.3). The ensuing eigenvalue problem is suitable for numerical calculation and appropriate shooting and Galerkin techniques are described in § 3.

Two examples are considered, those of uniform Eulerian-mean shear between wavy walls (§ 4) and of non-uniform Eulerian-mean shear beneath surface gravity waves (§ 5). In each case we solve the eigenvalue problem both with and without wave distortion. We find that the back effect of the mean flow modification upon the waves diminishes their catalytic action for all but the shortest waves and can, for sufficiently long waves, suppress the instability markedly. Further discussion is given in § 6.

2. Background

2.1. *The generalized Lagrangian-mean equations*

Andrews & McIntyre's (1978) generalized Lagrangian-mean equations are an exact and very general Lagrangian-mean description of the back effect of oscillatory distur-

† Craik (1970) deals with forced motions with oblique waves in $O(1)$ mean flows.

bances upon the mean state. The formulation is based upon an exact Lagrangian-mean operator $(\bar{})^L$, corresponding to any given Eulerian-mean operator $(\bar{})$, through an exact disturbance-associated particle displacement field $\boldsymbol{\xi}(\boldsymbol{x}, t)$ and is valid provided the mapping $\boldsymbol{x} \mapsto \boldsymbol{x} + \boldsymbol{\xi}$ is invertible. In consequence dependent variables are given an Eulerian description with position $\boldsymbol{x}$ and time t as independent variables. The Lagrangian-mean velocity $\bar{\boldsymbol{u}}^L$ is then the velocity field describing trajectories about which the fluctuating particle motions have zero mean, when *any* averaging process is applied.

For homentropic flows of constant density ρ in a non-rotating reference frame the GLM momentum equation is

$$\bar{\mathrm{D}}^L(\bar{u}_i^L - p_i) + \bar{u}_{k,i}^L(\bar{u}_k^L - p_k) + \pi_{,i} = -X_i, \tag{2.1}$$

where repeated indices imply summation, commas denote partial differentiation and $(x_1, x_2, x_3) \equiv (x, y, z)$. The operator $\bar{\mathrm{D}}^L$ is defined as $\bar{\mathrm{D}}^L = \partial/\partial t + \bar{u}_j^L \partial/\partial x_j$, and the vector wave property p_i, the pseudomomentum per unit mass, is

$$p_i = -\overline{\xi_{j,i} u_j^\ell}, \tag{2.2}$$

with $\bar{\mathrm{D}}^L \xi_j = u_j^\ell$. Finally X_i are dissipative terms while

$$\pi = \frac{\bar{\mathscr{P}}^L}{\rho} + \bar{\Phi}^L - \frac{1}{2}\langle u_j^\xi u_j^\xi \rangle,$$

where $\boldsymbol{u}^\xi$ is the actual fluid velocity and Φ^L is the force potential per unit mass.

We shall restrict attention to inviscid fluids (so X_i is identically zero) in which all mean quantities except possibly the mean pressure $\bar{\mathscr{P}}$ are independent of the streamwise direction; then, with $\Phi^L = 0$, $\pi_{,1}$ reduces to $\bar{\mathscr{P}}_{,1}^L$.

2.2. *Arbitrarily strong shear and $O(\epsilon)$ waves*

We consider the interaction between an $O(\epsilon^s)$ primary shear flow ($s \geqslant 0$) and two-dimensional straightcrested periodic waves that propagate in (or opposite to) the direction of the primary flow. Then with space coordinates (x, y, z), and in a reference frame that moves in the x-direction with the phase speed of the waves c_r^w, which is not sought as part of the solution, our primary shear flow is $\bar{\boldsymbol{u}}^L = [\bar{u}(z), 0, 0]$, where $\bar{u} = U(z) - c_r^w$ and $U(z)$ is the Eulerian-mean velocity profile in $[z_1, z_2]$. The waves are spanwise-independent and of constant amplitude with slope characterized by the small parameter ϵ; so provided the primary flow is free of critical layers ($\bar{u} = 0$), then the temporal growth or decay rate of the waves $\alpha c_i^w = 0$ and they induce an $O(\epsilon^2)$ pseudomomentum field $\boldsymbol{p} = [p_1, 0, 0]$.

We now envisage a small spanwise-periodic perturbation with streamwise-averaged Eulerian velocity components of the form

$$(\tilde{u}, \tilde{v}, \tilde{w}) = \delta \mathrm{Re}\{\mathrm{e}^{\sigma t}\mathrm{e}^{\mathrm{i}ly}[\hat{u}(z), -\epsilon^n \mathrm{i}\hat{v}(z), \epsilon^n \hat{w}(z)]\}, \tag{2.3}$$

which, provided the amplitude field of the waves is steady, satisfy continuity correct to $O(\epsilon^2)$ as (cf. Longuet-Higgins 1953; McIntyre 1988)

$$l\hat{v} + \hat{w}_{,3} = 0. \tag{2.4}$$

Here σ is the growth rate of the spanwise perturbation and δ is a second small parameter that measures the strength of this motion relative to the primary shear flow; δ is assumed sufficiently small that linearization with respect to δ yields a good approximation to the equations governing the spanwise periodic disturbance. For

instability, (2.1) and (2.4) must admit non-trivial solutions for boundary conditions of the form $\hat{w} = 0$ at $z = z_1, z_2$; and that requires $n = (2 - s)/2$ (see C*b*; Phillips 1993). Velocity perturbations in the y- and z-directions may therefore be weaker, by a factor of ϵ^n, than the x-velocity perturbation; likewise $\sigma = \epsilon^{\frac{s}{2}+1}\sigma_1$. So $n = 1$ for an $O(1)$ shear and (2.1) and (2.4) reduce to

$$\sigma_1 \hat{u} = -\hat{w}\bar{u}', \tag{2.5}$$

$$\hat{w}_{,33} + l^2\left[\frac{P^0_{1,3}\bar{u}'}{\sigma_1^2} - 1\right]\hat{w} = -\frac{l^2\bar{u}'}{\sigma_1}\hat{P}_1. \tag{2.6}$$

Here the prime denotes d/dz and $\mathrm{Re}\{\mathrm{e}^{ily}\hat{P}_1\}$ is the spanwise-periodic perturbation of pseudomomentum,

$$p_1 = \epsilon^2 P_1^0 + \epsilon^2\delta\mathrm{Re}\{\mathrm{e}^{\sigma t}\mathrm{e}^{ily}\hat{P}_1(z)\} + O(\epsilon^4, \epsilon^3\delta, \epsilon^2\delta^2), \tag{2.7}$$

that arises because the emerging secondary Eulerian velocity field distorts the primary wave field.

Wave distortion of this form is negligible in $O(\epsilon)$ or weaker shear flows but plays a role in stronger shear. Our object is to determine that role and in particular to find whether it, through $\hat{P}_1$, acts to enhance or inhibit instability.

The instability is manifested as longitudinal vortices, so of particular interest is the streamwise component of the vorticity-associated vector field $(\bar{u}_3^L - p_3)_{,2} - (\bar{u}_2^L - p_2)_{,3}$, which, because the y- and z-components of Stokes drift and pseudomomentum are zero here, is simply the mean longitudinal vorticity, $\tilde{\Omega} = \epsilon\delta\mathrm{Re}\{\mathrm{e}^{\sigma t}\mathrm{e}^{ily}\hat{\Omega}(z)\}$ where

$$\hat{\Omega}(z) = \frac{\sigma_1}{l\bar{u}'}\left[\hat{u}'' + T_1\hat{u}' + T_2\hat{u}\right] \tag{2.8}$$

with

$$T_1(z) = -\frac{2\bar{u}''}{\bar{u}'}, \qquad T_2(z) = 2\left(\frac{\bar{u}''}{\bar{u}'}\right)^2 - \frac{\bar{u}'''}{\bar{u}'} - l^2.$$

2.3. *Craik's eigenvalue problem for $O(1)$ shear flows*

The GLM formulation provides no direct means of evaluating $\hat{P}_1$ so a separate examination of the wave field is necessary. To do so C*b* noted that since only the $O(\epsilon^2\delta)$ contribution to p_1 is required, the influence on the waves of the $O(\epsilon\delta)$ velocity components may be ignored, i.e. the significant part of the distortion of the wave field is due to the $O(\delta)$ spanwise-periodic x-velocity, $\tilde{u}$. We thus need consider only the linear theory of wave motion in the presence of our Eulerian mean flow $\bar{u} + \tilde{u}$.

Such circumstances and the x-averaged flow field (2.3) suggest that the x-periodic perturbation field takes the form

$$\check{u}_i = \epsilon\mathrm{Re}\{\mathrm{e}^{\mathrm{i}\alpha x}[\phi'(z), 0, -\mathrm{i}\alpha\phi(z)]\}$$

$$+ \epsilon\delta\mathrm{Re}\{\mathrm{e}^{\sigma t}\mathrm{e}^{\mathrm{i}\alpha x}[\mathscr{U}_1(z)\cos ly, \mathscr{U}_2(z)\sin ly, \mathscr{U}_3(z)\cos ly]\} + O(\epsilon^2, \epsilon\delta^2), \tag{2.9}$$

where $\mathscr{U}_j$ are derived from the modification of the $O(\epsilon)$ wave field by the $O(\delta)$ spanwise-periodic component of u. To satisfy continuity

$$\mathrm{i}\alpha\mathscr{U}_1 + l\mathscr{U}_2 + \mathscr{U}_3' = 0,$$

while $\phi(z)$ and α denote the eigenfunction and wavenumber of the primary wave field which together satisfy Rayleigh's equation,

$$\bar{u}(\phi'' - \alpha^2\phi) - \bar{u}''\phi = 0. \tag{2.10}$$

P_1^0 and $\hat{P}_1$ must be recovered from (2.2). To do so we first obtain the particle displacements from (2.9) through $\bar{D}^L \xi_j = \breve{u}_j + \xi_k \bar{u}_{j,k}$. Substitution in (2.2) then yields at $O(\epsilon^2)$, *Ca*

$$P_1^0 = -\frac{\bar{u}}{2}\left\{\left|\left(\frac{\phi}{\bar{u}}\right)'\right|^2 + \alpha^2\left|\frac{\phi}{\bar{u}}\right|^2\right\}, \tag{2.11}$$

and a cast of $O(\epsilon^2\delta)$ terms which describe $\hat{P}_1$. Then on defining $\hat{\phi}(z) = \mathrm{i}\alpha^{-1}\mathscr{U}_3(z)$, employing the continuity and momentum equations and eliminating $\mathscr{U}_i$, *Cb* finds

$$\hat{P}_1 = \mathscr{A}(z)\hat{u}(z) + \mathscr{B}(z)\hat{u}'(z) + \mathrm{Re}\{\mathscr{C}(z)\hat{\phi}(z) + \mathscr{D}(z)\hat{\phi}'(z)\}, \tag{2.12}$$

where $\mathscr{A}$, $\mathscr{B}$, $\mathscr{C}$ and $\mathscr{D}$ are functions which are independent of σ. Specifically

$$\mathscr{A}(z) = \frac{|\phi'|^2}{2\bar{u}^2}\frac{\alpha^2+3l^2}{\alpha^2+l^2} + \frac{|\phi|^2}{2\bar{u}^2}(\alpha^2 + \frac{3\bar{u}'^2}{\bar{u}^2}) - \frac{\bar{u}'(|\phi|^2)'}{2\bar{u}^3}\frac{2\alpha^2+3l^2}{\alpha^2+l^2},$$

$$\mathscr{B}(z) = \frac{\alpha^2}{2(\alpha^2+l^2)}\left(\frac{|\phi|^2}{\bar{u}^2}\right)',$$

$$\mathscr{C}(z) = -\frac{\alpha^2\phi^*}{\bar{u}} + \frac{\alpha^2\bar{u}'}{\bar{u}(\alpha^2+l^2)}\left(\frac{\phi^*}{\bar{u}}\right)',$$

$$\mathscr{D}(z) = \frac{-\alpha^2}{\alpha^2+l^2}\left(\frac{\phi^*}{\bar{u}}\right)',$$

where * denotes conjugation. Moreover $\hat{\phi}(z)$ relates to the $O(\epsilon\delta)$ spanwise-periodic wave field modification and satisfies the Rayleigh–Craik equation,

$$\bar{u}\left[\frac{\mathrm{d}^2}{\mathrm{d}z^2} - (\alpha^2+l^2)\right]\hat{\phi} - \bar{u}''\hat{\phi} = -\hat{u}\left[\frac{\mathrm{d}^2}{\mathrm{d}z^2} - (\alpha^2+l^2)\right]\phi + \hat{u}''\phi. \tag{2.13}$$

Thus given the primary Eulerian-mean shear flow $\bar{u}(z)$, the primary wave-field eigenfunction $\phi(z)$ and appropriate boundary conditions, the eigenvalue problem for σ_1 is completely specified by the coupled system (2.5), (2.6) and (2.13) together with (2.11) and (2.12).

Finally, *Cb* showed that further analytical progress is possible when $l^2 \gg \alpha^2$ and $\alpha = O(1)$; then non-trivial solutions to (2.5), (2.6) and (2.13) with homogeneous boundary conditions exist provided

$$\mathrm{Im}\left\{\int_{z_1}^{z_2}(1+\lambda_k)^{1/2}\mathrm{d}z\right\} = \frac{N\pi}{l} \qquad (k = 1, 2), \tag{2.14}$$

for some integer N. Here

$$\lambda_{1,2} = \tfrac{1}{2}\{-\sigma_1^{-2}(G+H) \pm [\sigma_1^{-4}(G+H)^2 - 8\sigma_1^{-2}H]^{\frac{1}{2}}\},$$

$$H(z) \equiv \frac{\alpha^2\bar{u}'^2|\phi|^2}{\bar{u}^2} \quad \text{and} \quad G(z) \equiv -\alpha^2\bar{u}'\left(\frac{|\phi|^2}{\bar{u}}\right)'.$$

3. Numerical procedure

Two independent numerical approaches, a shooting method and a Galerkin technique, were used to solve the coupled system (2.5), (2.6) and (2.13). The shooting scheme employed fourth-order Runge–Kutta and began at $z = z_1$, where $\hat{w}$ and $\hat{\phi}$

are known, the object being to find values of $\hat{w}'$ and $\hat{\phi}'$ at the same point that lead to known boundary conditions at $z = z_2$. When that is so the chosen values of l, σ_1 and α, all assumed real (see later), are eigenvalues. To reduce the scope of our search we began by setting $\alpha = \sigma_1 = 1$ and stepped l in small increments over $O(1)$. Choosing appropriate pairs of $\hat{w}'$ and $\hat{\phi}'$ at $z = z_1$, however, was more involved. Here we began by placing the centroid of an equilateral triangle at a chosen point in $(\hat{w}', \hat{\phi}')$-space and, for given l, solved the coupled system with the pair $(\hat{w}', \hat{\phi}')$ at each vertex on the triangle. The centroid of the triangle was then moved to the vertex at which $\vartheta = |\hat{w}(z_2)| + |\hat{\phi}(z_2)|$ was (for the case of homogeneous boundary conditions) smallest and, after reducing the size of the triangle, the process was repeated. This procedure continued until ϑ fell below a prescribed minimum, which corresponded to an eigensolution. Of course the first triplet found need not lie on the $\sigma_1(l;\alpha)$ surface of greatest growth rate, because a hierachy of eigenvalues σ_1 exist for each l. So our options were (i) to fix l and increase σ_1 until its maximum was found, or (ii) since σ_1 increases monotonically with l (see §§ 4, 5), fix σ_1 and determine the smallest l corresponding to it. For computational reasons the second option proved easier and so the calculation continued until no smaller value of l could be found. Finally, using the previous solution as a starting point, eigensolutions to adjacent points on the $\sigma_1(l;\alpha)$ surface readily followed.

Our second approach solved for σ_1 directly for specified α and l and employed a Galerkin-type method. Here we first utilize (2.5) to write (2.6) in the form

$$\hat{u}_{,33} + T_1\hat{u}_{,3} + T_2\hat{u} + \sigma_1^{-2}(T_3\hat{u} + T_4\hat{P}_1) = 0 \tag{3.1}$$

where

$$T_3(z) = l^2 P^0_{1,3}\bar{u}', \qquad T_4(z) = -(l\bar{u}')^2.$$

Thus, since (3.1) is real, the eigenvalues σ_1 may be real, imaginary or complex conjugate pairs. The functions $\hat{u}$ and $\hat{\phi}$ are expanded in linearly independent, complete sets of basis functions u_i and ϕ_i that satisfy appropriate (see later) boundary conditions, so

$$\hat{u}_N(z) = \sum_{i=1}^{N} b_i u_i(z), \qquad \hat{\phi}_N(z) = \sum_{i=1}^{N} b_{N+i}\phi_i(z), \tag{3.2}$$

such that

$$\hat{P}_{1N}(z) = \sum_{i=1}^{N} \left[b_i(\mathscr{A} + \mathscr{B}\mathrm{D})u_i + b_{N+i}\mathrm{Re}\{(\mathscr{C} + \mathscr{D}\mathrm{D})\phi_i\}\right]; \tag{3.3}$$

here $\mathrm{D} = \mathrm{d}/\mathrm{d}z$ and b_i are constants that will be chosen to satisfy the differential equations (2.13) and (3.1). Substituting (3.2),(3.3) into (2.13),(3.1) then yields the residuals

$$R_1(\{b_i\}, z) =$$

$$\sum_{i=1}^{N} \left[b_i(\mathrm{D}^2 + T_1\mathrm{D} + T_2 + \sigma_1^{-2}T_3 + \sigma_1^{-2}T_4(\mathscr{A} + \mathscr{B}\mathrm{D}))u_i + b_{N+i}\sigma_1^{-2}T_4\mathrm{Re}\{(\mathscr{C} + \mathscr{D}\mathrm{D})\phi_i\}\right], \tag{3.4}$$

and

$$R_2(\{b_i\}, z) = \sum_{i=1}^{N} \left[b_i(T_5 + T_6\mathrm{D}^2)u_i + b_{N+i}[\bar{u}(\mathrm{D}^2 - \alpha^2 - l^2) - \bar{u}'']\phi_i\right], \tag{3.5}$$

where $T_5(z) = [\mathrm{D}^2 - \alpha^2 - l^2]\phi$ and $T_6(z) = -\phi$. The residuals and each of the approximating functions are required to be orthogonal as

$$\langle R_1, u_j \rangle = \langle R_2, \phi_j \rangle = 0; \quad j = 1, 2, ...N,$$

where

$$\langle f, g \rangle = \int_{z_1}^{z_2} f(z)g(z)\mathrm{d}z.$$

This leads to $2N$ linear, homogeneous algebraic equations for b_i which can be written in the form

$$\mathscr{L} = \sigma_1^{-2}\mathscr{M}, \tag{3.6}$$

where

$$\mathscr{L} = \begin{pmatrix} \boldsymbol{L}_{11} & 0 \\ \boldsymbol{L}_{21} & \boldsymbol{L}_{22} \end{pmatrix}, \qquad \mathscr{M} = \begin{pmatrix} \boldsymbol{M}_{11} & \boldsymbol{M}_{12} \\ \mathbf{0} & \mathbf{0} \end{pmatrix}.$$

Here $\boldsymbol{L}_{ij}$, $\boldsymbol{M}_{ij}$ and zero entries are all $N \times N$ matrix blocks, with

$$\begin{aligned}
(L_{11})_{ij} &= \langle u_i, (\mathrm{D}^2 + T_1\mathrm{D} + T_2)u_j \rangle, \\
(L_{21})_{ij} &= \langle \phi_i, (T_5 + T_6\mathrm{D}^2)u_j \rangle, \\
(L_{22})_{ij} &= \langle \phi_i, [\bar{u}(\mathrm{D}^2 - \alpha^2 - l^2) - \bar{u}'']\phi_j \rangle, \\
(M_{11})_{ij} &= \langle u_i, [T_3 + T_4(\mathscr{A} + \mathscr{B}\mathrm{D}]u_j \rangle, \\
(M_{12})_{ij} &= \langle u_i, T_4\mathrm{Re}\{(\mathscr{C} + \mathscr{D}\mathrm{D})\phi_j\} \rangle.
\end{aligned}$$

Non-zero solutions to (3.6) exist if and only if the determinant of the coefficients vanishes, namely

$$\det(\mathscr{L} - \sigma_1^{-2}\mathscr{M}) = 0. \tag{3.7}$$

Moreover because (3.7) is a $2N$th-order polynomial equation, an N-term Galerkin expansion produces the first $2N$ among the infinite number of eigenvalues of the system (3.6).

Of interest is the largest real value of σ_1 for each pair (α, l) and the eigenfunctions $\hat{u}$ and $\hat{\phi}$. Chebyshev polynomials were used as basis functions. The accuracy provided by the $N = 15$ expansion was considered adequate for our purposes for the problem of §4 and $N = 20$ for the problem for §5. All computations were performed on a DECstation 5000/200 using double precision arithmetic with IMSL routines to solve the eigenvalue problem (3.6). Both the shooting and Galerkin approach yielded results identical to five decimal places. But although useful as a cross-check, the shooting method lacked the specificity of the Galerkin approach and was restricted to isolating real eigenvalues, σ_1; and as the project developed the Galerkin approach came to be used exclusively. The Galerkin program was written in mixed Fortran and C and ran very efficiently. But while a timescale of minutes was sufficient to generate the information to produce figure 1 say, figure 8 required a timescale of days.

4. Uniform shear between wavy walls

As our first example we consider a uniform Eulerian-mean shear flow $\bar{u} = z$ in $[z_1, z_2]$ with $z \neq 0$, upon which is superposed a two-dimensional wave-like disturbance $\alpha\phi = \gamma\exp(-\alpha z)$ which satisfies (2.10). We assume that the disturbance is brought about by rigid wavy walls at z_1 and z_2, so $\hat{\phi} = \hat{w} = 0$ on each wall. *Cb* has shown that this interaction leads to instability over some $(\alpha, l; \gamma)$; but what is unclear is how

wave distortion affects that instability. We thus consider the problem both with and without wave distortion over $[z_1, z_2] = [1, 2]$.

4.1. *No wave distortion*

When wave distortion is ignored, we need solve only (2.6) with $\hat{P}_1 = 0$,

$$\bar{u}' P^0_{1,3} = \frac{\Lambda e^{-2\alpha z}}{z^4}(1 + 2\alpha z + 2\alpha^2 z^2 + \tfrac{4}{3}\alpha^3 z^3), \qquad \Lambda = \frac{3\gamma^2}{2\alpha^2} \tag{4.1}$$

(from (2.11)) and the boundary conditions $\hat{w}(z_1) = \hat{w}(z_2) = 0$. There is no general solution, but the problem is tractable in the following limiting situations. Before treating them, however, we note that because σ_1 occurs always as the ratio σ_1/γ we set, with no loss of generality, $\gamma = 1$.

In the first limit $l^2 \gg \alpha^2$, $\alpha = O(1)$ and here two linearly independent solutions may be constructed via the WKBJ approximation. Equivalently we may set $H(z) = 0$ and replace $G(z)$ with $\bar{u}' P^0_{1,3}$. Then $\lambda_{1,2} = -\frac{1}{2}\sigma_1^{-2} G[1 \pm 1]$, so $\lambda_{1,2}$ are real provided σ_1 is real and the integrand in (2.14) is imaginary (and so non-trivial solutions exist) only if $-\lambda_1 = \sigma_1^{-2} G$ is greater than unity. The largest upper bound for σ_1 is then seen to occur when G is maximum (in this instance at $z = 1$) and $-\lambda_1$ is minimum, i.e. approaching unity from above, indicating

$$\sigma_1 \sim \Lambda^{\frac{1}{2}} e^{-\alpha}(1 + 2\alpha + 2\alpha^2 + \tfrac{4}{3}\alpha^3)^{\frac{1}{2}} \qquad (\alpha \neq 0, \quad l^2 \to \infty). \tag{4.2}$$

The second limit requires $|\alpha z| \ll 1$; then (2.6) becomes

$$\hat{w}_{,33} + l^2 \left[\frac{\Lambda}{\sigma_1^2 z^4} - 1 \right] \hat{w} = 0.$$

This is Mathieu's modified differential equation which can be transformed to the standard form (Abramowitz & Stegun 1964)

$$\frac{d^2 K}{d\theta^2} - (r - 2q \cosh 2\theta) K = 0$$

with $\hat{w} = z^{\frac{1}{2}} K(\theta)$ and $z = (\Lambda/\sigma_1^2)^{\frac{1}{4}} \exp\{(\theta + i\pi/4)\}$; it is subject to the boundary conditions $K = 0$ at both $\theta(z_1)$ and $\theta(z_2)$. Further $r = 0.25$ and $q = \mp i l^2 \Lambda^{\frac{1}{2}}/\sigma_1$. In this domain the most unstable real root $\sigma_1 \sim \Lambda^{\frac{1}{2}} l/2$ as $l \to 0$ and, in accord with (4.2), $\sigma_1 \sim \Lambda^{\frac{1}{2}}$ as $l \to \infty$. Thus the magnitude of σ_1 increases with l from zero when l equals zero to a constant given by (4.2) as $l^2 \to \infty$; concurrently σ_1 varies inversely with α for all l. Details over a wider range of αz are provided by our numerical solution, which is, of course, in accord with the above results, as we see in figures 1 and 4.

4.2. *Wave distortion*

We now allow the wave field to distort and begin our study by looking at the limit $l^2 \to \infty$. Here, for $\alpha = O(1)$,

$$G + H = \frac{2\gamma^2 e^{-2\alpha z}}{z^2}(\alpha z + 1)$$

and is real. But unlike the former example, and even though we limit our search to real eigenvalues σ_1, it is evident that $\lambda_{1,2}$ are real only if

$$\sigma_1 \leqslant \frac{\gamma e^{-\alpha z}}{\sqrt{2z}}(\alpha z + 1) \qquad (\alpha = O(1)).$$

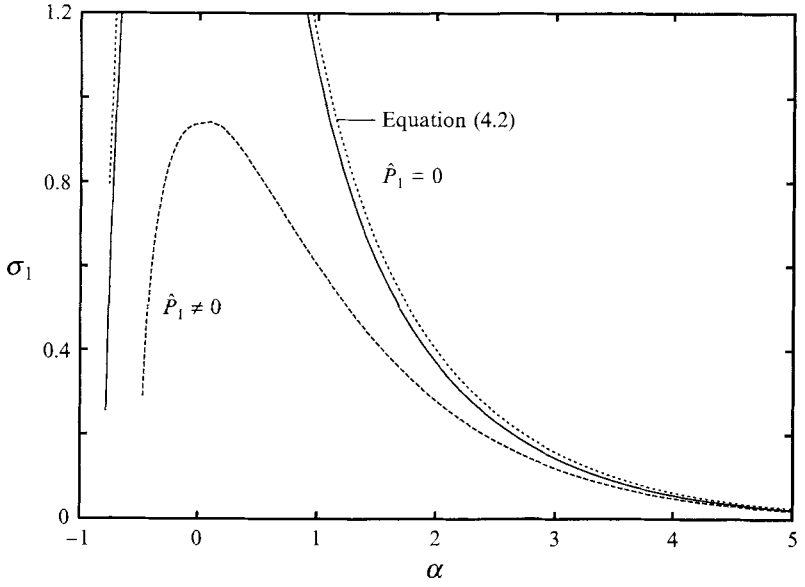

FIGURE 1. Curves of σ_1 against α in the limit $l^2 \to \infty$, both with and without wave distortion.

When $\lambda_{1,2}$ are real, C*b* has shown that instability occurs whenever $\alpha z > 0$ or $-1 < \alpha z < 0$ throughout the flow, but not when $\alpha z < -1$ throughout the flow.

Unfortunately, solving (2.14) to determine the σ_1-upper bound proved quite a challenge and we eventually succumbed to the simpler numerical solution of (2.13) and (3.1). To lend credibility to the calculation we replaced $\hat{P}_1$ with $b\hat{P}_1$ and first considered the case $b \to 0$. Doing so, also with $\gamma = 1$, recovered (4.2) as it should. Setting $b = 1$ then yielded the asymptote given in figure 1, which depicts σ_1 values well into the range for which $\lambda_{1,2}$ are complex.

C*b* did not investigate such cases, but his results for real $\lambda_{1,2}$ are representative of complex $\lambda_{1,2}$: specifically, instability occurs whenever the local wave amplitude $|\phi|$ everywhere *decreases* in the direction of increasing speed of the primary flow $\bar{u}$ relative to the wave, i.e. $\alpha z > 0$ throughout the flow. However when the wave amplitude $|\phi|$ everywhere *increases* in the direction of increasing speed $|\bar{u}|$, instability occurs only when the wave is sufficiently long that $|\alpha z| < 0.5$ throughout $[z_1, z_2]$ – in contrast to $|\alpha z| < 1$ for real $\lambda_{1,2}$ – and no such instability is evident for waves short enough that $|\alpha z| > 0.5$ everywhere in $[z_1, z_2]$. Moreover, the growth rate of the instability is a maximum when $|\phi|$ is everywhere constant throughout the flow, i.e. $\alpha z \to 0$ and the maximum is bounded.

Such behaviour is markedly different to the non-distortion case where σ_1 is unbounded as $\alpha z \to 0$ and the flow is unstable for all $\bar{u}' P^0_{1,3} > 0$. Indeed the distortion and non-distortion cases are asymptotically equivalent only as $\alpha z \to +\infty$. In the $l^2 \to \infty$ limit, therefore, and indeed for all l^2, it is evident that wave distortion plays an increasingly greater role as αz decreases from $+\infty$.

Of course ϕ is infinite when $\alpha = 0$, but we should like more detail as $\alpha \to 0$. We thus consider the case $l^2 \gg \alpha^2$, $\alpha \to 0$. Then with the rescaling $\hat{w} = \alpha \hat{w}^*$, $\hat{\phi} = \hat{\phi}^*$, (2.6) becomes

$$\hat{w}^*_{,33} + \frac{\gamma^2}{\sigma_1^2 z^3}\hat{w}^*_{,3} + l^2\left[\frac{\gamma^2}{\sigma_1^2 z^2} - 1\right]\hat{w}^* = \frac{\gamma}{\sigma_1 z}\left\{\left[l^2 + \frac{1}{z^2}\right]\hat{\phi}^* - \frac{1}{z}\hat{\phi}^*_{,3}\right\} \tag{4.3}$$

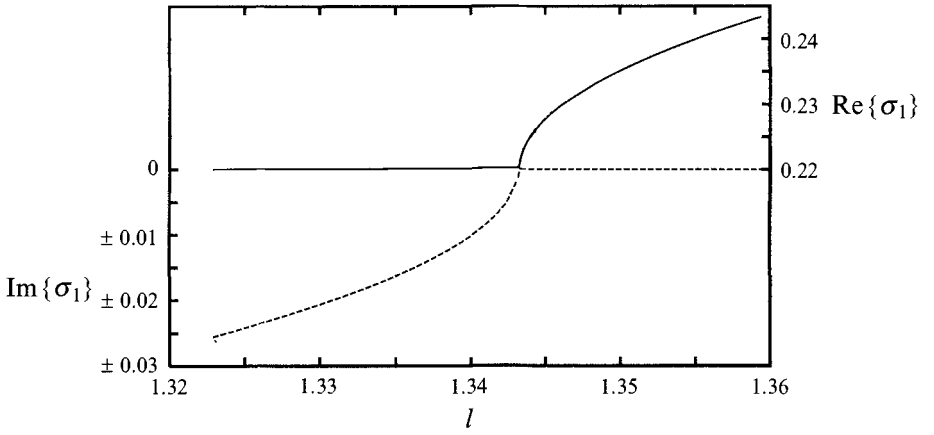

FIGURE 2. Real (solid line) and imaginary parts (dashed line) of the growth rate σ_1 in the long-wave limit $\alpha \to 0$, near $l = l_0$

with from (2.13)

$$\left[\frac{\mathrm{d}^2}{\mathrm{d}z^2} - l^2\right]\hat{\phi}^* = -\frac{\gamma}{\sigma_1 z}\left[\frac{\mathrm{d}^2}{\mathrm{d}z^2} + l^2\right]\hat{w}^*. \tag{4.4}$$

The eigenvalue problem (4.3), (4.4) for σ_1 is now a function only of l. On solving it using a Galerkin technique similar to that outlined in § 3, we find that σ_1 (the largest positive real eigenvalue) decreases monotonically with l from $\sigma_1 \sim 1$ in the limit $l^2 \to \infty$ to a real minimum not at $l = 0$ but, as we see in figure 2, at $l = l_R = 1.34350$. The eigenvalue σ_1 has no real roots over $0 \leqslant l < l_R$, only complex ones which appear at l_R as a Hopf bifurcation (see later). We thus ask whether $\sigma_1 = 0$ and $l = 0$ ever coexist?

Consider then the case $\alpha^2 \gg l^2$, $l \to 0$ and assume that.

$$\lim_{\substack{l\to 0\\ \sigma_1 \to 0}} \left(\frac{l}{\sigma_1}\right)^2 = \kappa^2;$$

on rescaling $\hat{\phi}^+ = \sigma_1 \hat{\phi}$ and $\hat{w}^+ = \hat{w}$, (2.6) and (2.13) become

$$\hat{w}^+_{,33} - \kappa^2\varrho^2\frac{\alpha z + 1}{\alpha^2 z}\hat{w}^+_{,3} + \kappa^2(P^0_{1,3} - \mathscr{A})\hat{w}^+ = \kappa^2\varrho\left[\left\{\alpha + \frac{\alpha z + 1}{z^2}\right\}\hat{\phi}^+ - \frac{\alpha z + 1}{\alpha z}\hat{\phi}^+_{,3}\right]$$

and

$$\left[\frac{\mathrm{d}^2}{\mathrm{d}z^2} - \alpha^2\right]\hat{\phi}^+ = -\frac{\varrho}{\alpha}\hat{w}^+_{,33}$$

with $\varrho = \gamma \mathrm{e}^{-\alpha z}/z$. Of interest are real positive α for which there exist real eigenvalues κ. Our results, also obtained using Galerkin techniques, indicate that real κ do exist for $\alpha \geqslant \alpha_R$, where $\alpha_R = 0.76350$, at which point $\kappa = \kappa_R \approx 2\pi$. But of the $2N$ roots for κ, only $2J$ are real and $2K$ are imaginary (J, K integer); the remainder are complex conjugate pairs. Specifically, $J = 0$ for $\alpha < \alpha_R$ and $K = 0$ for $\alpha > \alpha_I$, where $\alpha_I \approx -0.61$. Moreover $J = 1$ ($K = 1$) at $\alpha = \alpha_R+$ ($\alpha = \alpha_I-$) and increases with increasing (decreasing) α until eventually $J = N$ ($K = N$), at which point all the eigenvalues are real (imaginary). Finally, while the real parts of the complex conjugate pairs are positive when $N > J > 0$, they change from positive to negative in $\alpha_I \leqslant \alpha \leqslant \alpha_R$ and remain negative for $N > K > 0$. So on writing $\sigma_1 = \alpha c_i^v \mp \mathrm{i}\alpha c_r^v$, we

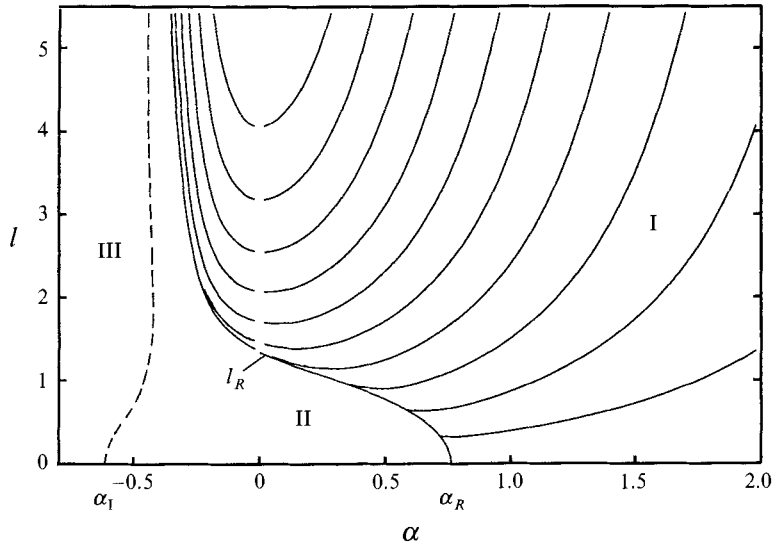

FIGURE 3. Contours of constant growth rate σ_1 in α–l space with stability boundaries along which σ_1 is not constant. The boundary connecting l_R to α_R separates instability to longitudinal vortex form (I) from that with alternating sign (II); the dashed curve separates II from a region which is stable to longitudinal vortex form (III).

must interpret the right-hand side of (2.3) as

$$\delta \mathrm{Re}\{e^{\alpha c_i^v t} e^{i(ly \mp \alpha c_r^v t)} [\hat{u}(z), -\epsilon i\hat{v}(z), \epsilon\hat{w}(z)]\}.$$

The curve connecting l_R to α_R is shown, with impinging contours of constant σ_1, in l–α space in figure 3. Note that the (l_R, α_R)-curve is not a line of constant σ_1 but rather a demarcation between eigenvalues for σ_1 for which $J = 0$ and $J = 1$. The (l_R, α_R)-curve also depicts marked suppression in catalytic action beyond that for $J \geqslant 1$ as shown in figure 4; so although the flow remains unstable to longitudinal vortex form on the long-wave side of the curve, the vortices are relatively weak rolls. On the $J \geqslant 1$ side of the curve, the instability is dominated by eigenmodes which are real; the real parts of the complex conjugate pairs are tertiary at best. But only complex conjugate pairs occur on the $J = 0$ side of the curve where the instability not only grows, so long as $\alpha c_i^v > 0$, but is subject to a standing oscillation owing to the $\pm\alpha c_r^v$ contribution: that is, the longitudinal vortices stand in space and alternate in sign (see § 6); there is also the possibility that a $+\alpha c_r^v$ or $-\alpha c_r^v$ alone each gives rise to spanwise propagating rolls with equal and opposite phase speed. Of course on fixing l on the (l_R, α_R)-curve and further decreasing α, we ultimately reach a point at which $\alpha c_i^v \leqslant 0$ for all eigenmodes; here the flow is neutrally stable to longitudinal vortex form. The neutral curve is depicted by dashes and indicates that $\alpha z \sim -0.5$ as $l^2 \to \infty$ and that $\alpha z = \alpha_I z$ when $l = 0$.

Figure 5 shows $\hat{u}$- and $\hat{\phi}$-eigenfunctions typical of those for any αz for which the flow is unstable to longitudinal vortex form. Observe that their complexity, measured in terms of the number of inflexion points or zeros, increases with l, or equally the level of instability, while the point of peak distortion (and maximum longitudinal vorticity) shifts toward the wall at which the primary mean velocity, relative to the wave, is minimum, i.e. $\bar{u}(z_1)$. Hence, because ϕ is a maximum at z_1 for $\alpha z > 0$, and a minimum there when $\alpha z < 0$, it is evident that the amplitude of the primary wave

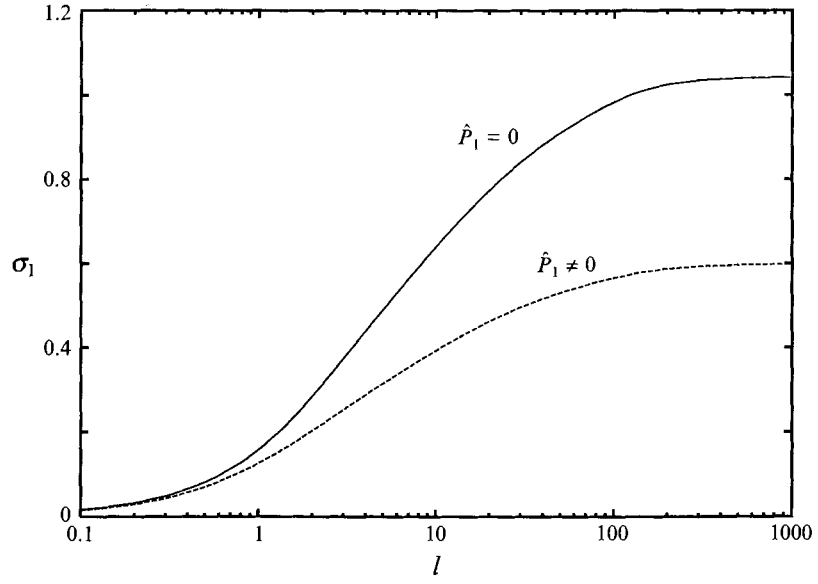

FIGURE 4. Variation of the growth rate σ_1 with l both with and without wave distortion, for $\alpha = 1$.

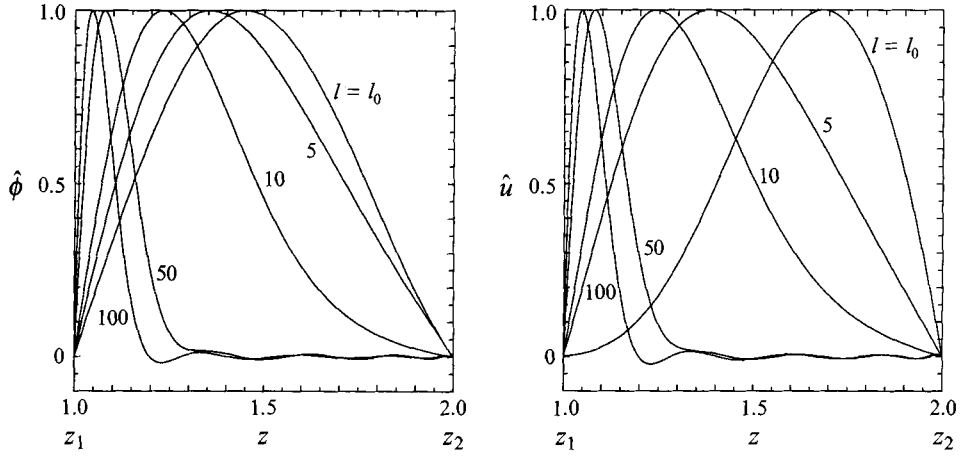

FIGURE 5. The eigenfunctions $\hat{\phi}(z)$ and $\hat{u}(z)$ for various values of l in the long-wave limit $\alpha \to 0$.

field plays little if any role in determining the location of the vortices, behaviour consonant with the waves acting solely as a catalyst to the instability.

Looking now in more detail, we see that $\hat{\phi}$ and $\hat{u}$ are much the same at each l and contain inflexion points only on the $z = z_2$ side of their peak, except in the vicinity of the (α_R, l_R)-curve and along $l = 0$, $\alpha > \alpha_R$ where catalytic action is greatly reduced. Here the $\hat{u}$-eigenfunction changes noticeably: first, an inflexion point occurs on the $z = z_1$ side of the peak; and second, we see that while $\hat{u}'(z_1) = 0$ for $\alpha \leqslant \alpha_R$ we have $\hat{u}'(z_1) > 0$ for $\alpha > \alpha_R$. Hence, while an appropriately placed inflexion point in the $\hat{u}$-eigenfunction is the hallmark of suppressed catalytic action and thus suppressed instability to longitudinal vortices, an appropriately placed turning point is necessary to incite vortices of alternating sign.

5. Non-uniform shear beneath surface gravity waves

As our second example we consider a unidirectional shear layer in the presence of $O(\epsilon)$ two-dimensional surface gravity waves that are independent of the spanwise direction. Craik (1977), C*b* and, for stratified flows, Leibovich (1977) & Leibovich and Paolucci (1981), have studied the interaction of such waves with $O(\epsilon)$ or weaker shear flows, but here the shear is $O(1)$. In lakes and oceans the shear is wind induced and its interaction with surface waves gives rise to longitudinal vortices known as Langmuir circulations. These are thought to be largely responsible for the formation of thermoclines and the maintenance of mixed layers in lakes; they also provide a wonderful elevator/descender mechanism for plankton and other marine organisms.

In such circumstances we expect the velocity profile $U(z)$ to decrease with depth from the mean free surface $z = z_2 = 0$ and thus assume

$$\bar{u} = c_r^w(\beta e^{hz} - 1) \qquad (h > 0) \tag{5.1}$$

over $-\infty < z \leqslant 0$; so to avoid critical layers $\beta < 1$, where $\beta = U(0)/c_r^w$, and c_r^w may be of either sign.

5.1. *Boundary conditions*

The position of the free surface is given by $z = \eta(x, y, t)$ and appropriate free-surface boundary conditions are continuity of pressure and the requirement that the free surface is a material surface of the fluid. So in the absence of surface tension,

$$\mathscr{P} = 0 \quad \text{and} \quad \frac{\mathrm{D}(z-\eta)}{\mathrm{D}t} = 0 \quad \text{on} \quad z = \eta, \tag{5.2}$$

while at large depth the fluid velocity must decay to zero,

$$\boldsymbol{u} \to [-c_r^w, 0, 0] \quad \text{as} \quad z \to -\infty. \tag{5.3}$$

In the undisturbed state, which is a solution to the boundary value problem given by (2.1), continuity and the boundary conditions (5.2) and (5.3), the fluid surface is planar (so $\eta = 0$), the pressure is given by the hydrostatic law $\mathscr{P} = -\rho g z$ and $\boldsymbol{u} = [\bar{u}, 0, 0]$. But with small, time-dependent three-dimensional perturbations, the velocity field is conveniently decomposed into the mean flow $\bar{u}$, $O(\delta)$ streamwise-averaged modifications to it $\tilde{u}$, and $O(\epsilon)$ fluctuations owing to the wave field $\check{u}$, whose streamwise average is zero. Thus $\boldsymbol{u} = [\bar{u} + \tilde{u} + \check{u}, \tilde{v} + \check{v}, \tilde{w} + \check{w}]$, with the pressure $\mathscr{P} = -\rho g z + \mathscr{P}_e$ and free surface $z = \eta_e$, although in order to express (5.2) and (5.3) at $O(\epsilon)$, $O(\delta)$ and $O(\epsilon\delta)$, $\mathscr{P}$ and η are best expanded in a form reminiscent of the velocity components (2.3), (2.9). Thus

$$\mathscr{P} = \mathscr{P}_0(z) + \epsilon\mathscr{P}_1(x, z) + \delta\mathscr{P}_2(x, y, z, t) + \epsilon\delta\mathscr{P}_3(x, y, z, t) + O(\epsilon^2\delta, \epsilon\delta^2),$$

$$\eta = \eta_0 + \epsilon\eta_1(x) + \delta\eta_2(y, t) + \epsilon\delta\eta_3(x, y, t) + O(\epsilon^2\delta, \epsilon\delta^2);$$

we also note that $\mathscr{P}_i = \rho g \eta_i$ for $i = 1, 2, \ldots$ on $z = 0$.

Rayleigh's equation (2.10) then follows by eliminating pressure from the $O(\epsilon)$ x- and z-momentum equations, while eliminating η_1 from the $O(\epsilon)$ version of (5.2) gives the free-surface boundary condition

$$\bar{u}^2\phi' - (\bar{u}\bar{u}' + g)\phi = 0 \quad \text{on} \quad z = 0, \tag{5.4}$$

while (5.3) requires at $O(\epsilon)$ that

$$\phi \to 0 \quad \text{as} \quad z \to -\infty. \tag{5.5}$$

Only the x-momentum equation appears at $O(\delta)$, as

$$\epsilon e^{\sigma t}(\sigma_1 \hat{u} + \hat{w}\bar{u}')\cos ly = -\frac{\partial \mathscr{P}_2}{\rho \partial x},$$

while from (5.2) at $O(\delta)$ $\partial \eta_2/\partial t = 0$ on $z = 0$. Thus in view of (2.5) and because $\eta_2 = 0$ at time $t = 0$, it and $\mathscr{P}_2$ remain zero for all time; in consequence we must proceed to $O(\epsilon\delta)$ to determine $\hat{u}(0)$.

$\hat{\phi}$ is an $O(\epsilon\delta)$ quantity, and to analyse events at this order we must decompose η_3 into an x-averaged and x-periodic part, namely $\eta_3 = \mathrm{Re}\{e^{\sigma t}\cos ly(a + be^{i\alpha x})\}$. Eliminating η_3 from the $O(\epsilon\delta)$ form of the free-surface boundary conditions (5.2), and noting $\sigma = \epsilon\sigma_1$, then yields the boundary conditions $\hat{u}(0) = 0$ and

$$\frac{\alpha^2}{\alpha^2 + l^2}\bar{u}^2\hat{\phi}' - \left(\frac{\alpha^2}{\alpha^2 + l^2}\bar{u}\bar{u}' + g\right)\hat{\phi} = \frac{\alpha^2}{\alpha^2 + l^2}\bar{u}\hat{u}'\phi \quad \text{on} \quad z = 0,$$

which describes the distortion of the wave amplitude at the free surface due to an $O(\delta)$ axial velocity modification to the primary shear flow. Note, however, that $\hat{\phi}(0) = 0$ for $l^2 \gg \alpha^2$ which constitutes the major portion of our domain of interest; for the purpose of our calculations, therefore, we shall permit wave distortion only in the interior. Finally, at large depth, we see from (2.3) and (2.9) that at $O(\epsilon\delta)$ (5.3) requires

$$\hat{w} \to 0 \quad \text{and} \quad \hat{\phi} \to 0 \quad \text{as} \quad z \to -\infty.$$

Boundary conditions appropriate to our coupled system (2.13), (3.1), therefore, are two homogeneous Dirichlet conditions at $z = z_1$ and two at $z = z_2$. We shall consider two cases: the first (§ 5.3) excluding wave field distortion, the second (§ 5.4) permitting it. But before proceeding we require a wave field compatible with (5.1).

5.2. *Primary wave field*

Such a primary wave field follows on noting that (5.1), (2.10) and the substitutions

$$\alpha\phi = \zeta^{\frac{\alpha}{h}}\chi(\zeta), \quad \zeta = \beta e^{hz},$$

lead directly to the hypergeometric equation

$$\frac{d^2\chi}{d\zeta^2} + \frac{(1 + 2\alpha/h)}{\zeta}\frac{d\chi}{d\zeta} - \frac{\chi}{\zeta(\zeta - 1)} = 0 \quad \text{for} \quad \zeta \in (0, \beta].$$

So provided $|\beta| < 1$, then $|\zeta| < 1$ and the solution is

$$\chi = A_1 F(a, b; c; \zeta) + A_2 \zeta^{1-c} F(a - c + 1, b - c + 1; 2 - c; \zeta), \tag{5.6}$$

where $F(a, b; c; \zeta)$ is the hypergeometric series (Abramowitz & Stegun 1965),

$$a = \frac{\alpha}{h} + \left(\frac{\alpha^2}{h^2} + 1\right)^{\frac{1}{2}}, \quad b = \frac{\alpha}{h} - \left(\frac{\alpha^2}{h^2} + 1\right)^{\frac{1}{2}}, \quad c = 1 + \frac{2\alpha}{h},$$

and A_1, A_2 are constants. We shall set $A_1 = \gamma$ and to ensure $\chi(\zeta)$ is bounded, $A_2 = 0$; then

$$\alpha\phi = \gamma\zeta^{\frac{\alpha}{h}}F(a, b; c; \zeta) \quad \text{for} \quad \zeta \quad \text{in} \quad (0, \beta], \tag{5.7}$$

in accord with (5.5) which requires $\phi \to 0$ as $\zeta \to 0$. Note that because the wave phase speed is not sought as part of our solution we may disregard the free-surface boundary condition (5.4).

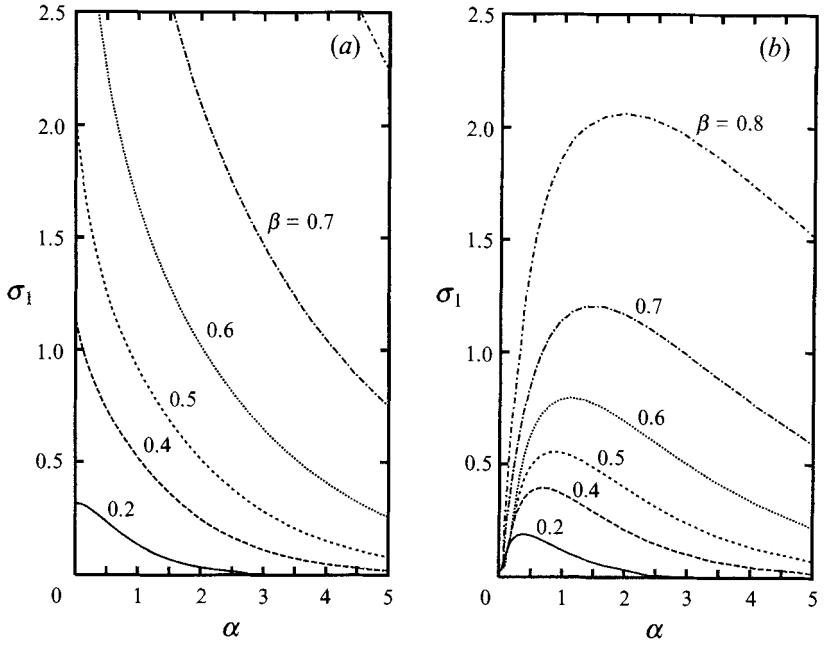

FIGURE 6. Curves of σ_1 against α for various values of β in the limit $l^2 \to \infty$: (*a*) without wave distortion; (*b*) with wave distortion.

Straightforward analysis then yields the product $\bar{u}'P^0_{1,3}$; on factoring out the largest singularity we find

$$\bar{u}'P^0_{1,3} = \frac{|\zeta|^{\frac{2\alpha}{h}+1}h}{2(1-\zeta)^4}(\alpha S_1 + hS_2),$$

where the functions $S_i(\zeta;\alpha)$ $(i = 1,4)$ are real and smooth in $|\zeta| < 1$. Specifically

$$S_1 = \zeta(\zeta + 2|\zeta|(1-\zeta))S_3^2 + 2(1-\zeta)^2(\zeta + 2|\zeta|)\chi S_3 - 4(\zeta-1)^3\chi^2,$$

$$S_2 = |\zeta|(\zeta^2+2)S_3^2 + 2|\zeta|(1-\zeta)\chi S_3 + 2\zeta|\zeta|(1-\zeta)(\zeta S_3 + \chi(1-\zeta))\frac{\mathrm{d}S_3}{\mathrm{d}\zeta} - 2|\zeta|(1-\zeta)^2\chi^2,$$

with

$$S_3 = \zeta(\zeta-1)\left(\frac{h}{\alpha}\frac{\mathrm{d}^2\chi}{\mathrm{d}\zeta^2} + \frac{2}{\zeta}\frac{\mathrm{d}\chi}{\mathrm{d}\zeta}\right).$$

Note that S_3, $\mathrm{d}S_3/\mathrm{d}\zeta$ and thus $\bar{u}'P^0_{1,3}$ are bounded as $\alpha \to 0$.

5.3. *No wave-field distortion*

Consider first the case without wave distortion. Here we need solve only (2.6) with $\hat{P}_1 = 0$ and the boundary conditions $\hat{w}(z_1) = \hat{w}(z_2) = 0$. Then in ζ-variables, and on writing $\hat{w} = \zeta^{-\frac{1}{2}}W$, (2.6) becomes

$$\frac{\mathrm{d}^2W}{\mathrm{d}\zeta^2} + \frac{1}{\zeta^2}\left(\frac{l^2}{h^2}\left[\frac{\bar{u}'P^0_{1,3}}{\sigma_1^2} - 1\right] + \frac{1}{4}\right)W = 0 \quad \text{for} \quad \zeta \in (0,\beta].$$

Two linearly independent solutions for W may be constructed via the WKBJ approximation as $(l/h)^2 \to \infty$. On setting $H = 0$ and $G = \bar{u}'P^0_{1,3}$, these satisfy the boundary conditions $W(0) = W(\beta) = 0$ provided (2.14) is satisfied. Then $\lambda_{1,2}$ is real provided σ_1

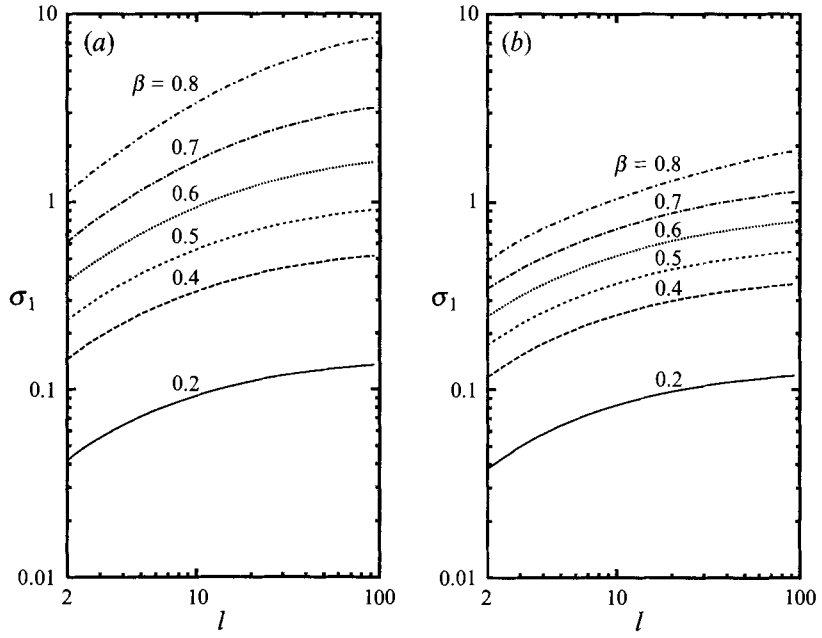

FIGURE 7. Curves of σ_1 against l for $\alpha = 1$ at various values of β: (*a*) without wave distortion; (*b*) with wave distortion.

is real and the largest upper bound for σ_1 is seen to be

$$\sigma_1 \sim |\beta|^{\frac{8}{7}} h^{\frac{1}{2}} (\alpha s_1 + h s_2)^{\frac{1}{2}} \quad \text{as} \quad \left(\frac{l}{h}\right)^2 \to \infty, \tag{5.8}$$

where $s_i = |\beta|(\beta - 1)^{-4} S_i(\beta; \alpha)/2 \quad (i = 1, 2)$.

Thus the flow is unstable to longitudinal vortex form (at least for $0 < |\beta| < 1$) provided $\alpha s_1 + h s_2 > 0$, the growth rate increasing dramatically as $\beta \to 1$. Furthermore σ_1 is bounded as $\alpha \to 0$ (in contrast to our previous example) and, because $\lim_{\alpha \to \infty} (\alpha^{\frac{1}{2}} \beta^{\alpha}) \to 0$ for $\beta < 1$, diminishes to zero as $\alpha \to \infty$.

Further details are given by the numerical solution in which we set $\gamma = h = 1$ and confine attention to the finite domain $-1 \leqslant z \leqslant 0$. Results as $l^2 \to \infty$ for various values of positive β are depicted in figure 6*a* and are in accord with the aforementioned asymptotic behaviour. The variation of σ_1 with l is given in figure 7*a*; as in the previous example (§ 4.1), σ_1 increases uniformly from zero at $l = 0$ to a finite upper bound as $l^2 \to \infty$.

5.4. *Wave-field distortion*

Allowing the wave field to distort again plays little role for sufficiently large α, but causes a marked diminution in growth rate as $\alpha \to 0$, as we see in figure 6*b*. The diminution is further accentuated as β increases (figures 6*b* and 7*b*), an occurrence reflected by the placement (in α, l-space) of the boundary separating eigenvalues for σ_1 for which $J = 0$ and $J = 1$ (see § 4); figure 8. In short, as β increases, a progressively larger portion of (α, l)-space is subject to standing longitudinal vortices which alternate in sign.

Looking now to the eigenfunctions, figure 9, we see that they depict much the same features of those in our earlier problem (§ 4.2): (i) as σ_1 increases, the peak,

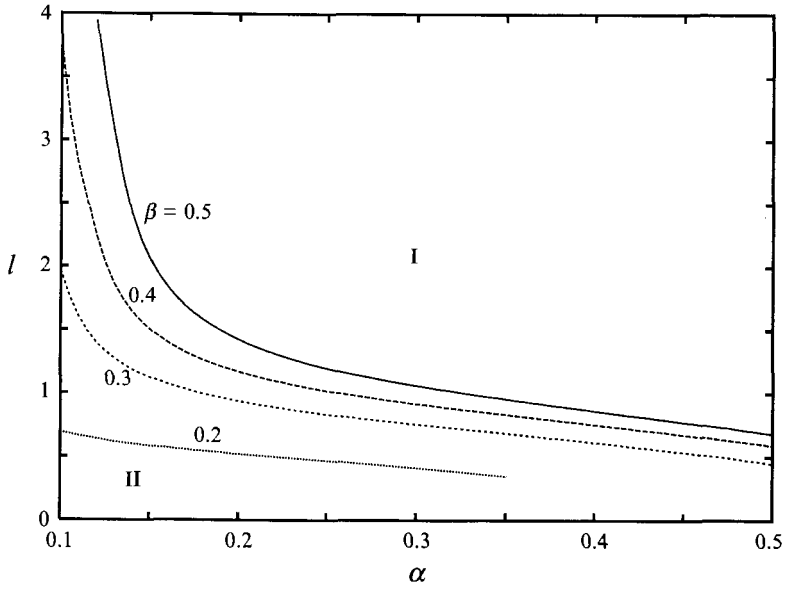

FIGURE 8. Boundaries separating regions unstable to longitudinal vortex form (I) from that with alternating sign (II) for various values of β in (α, l)-space.

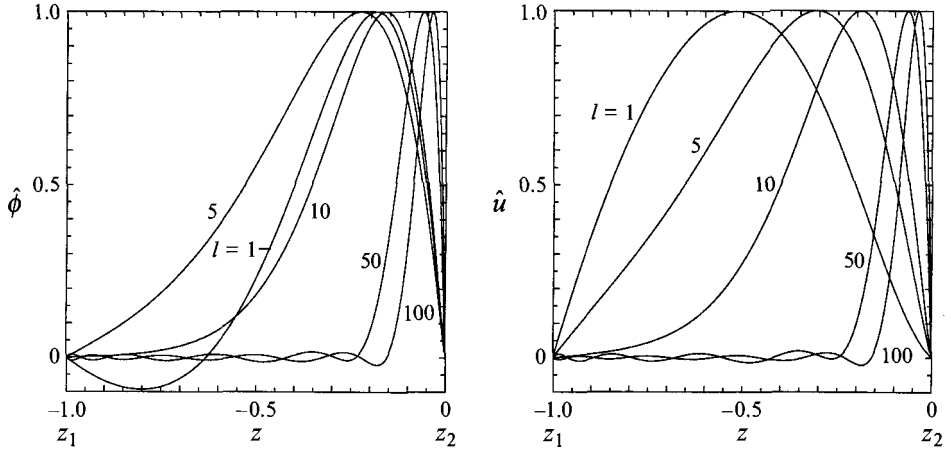

FIGURE 9. The eigenfunctions $\hat{\phi}(z)$ and $\hat{u}(z)$ for various values of l for $\alpha = 1$ and $\beta = 0.5$.

and thus the location of the vortices, shifts toward the boundary (in this case the free surface $z = z_2$) at which the mean velocity $\bar{u}$ relative to the wave, is minimum; (ii) the eigenfunctions exhibit an inflexion point on the z_1 side of the peak except when a marked suppression in catalytic action occurs; (iii) the vortices stand but alternate in sign or propagate spanwise (see §§4.2,6) when a turning point occurs in the $\hat{u}$-eigenfunction at z_2. Further, when standing oscillations first occur, the $\hat{u}$-eigenfunctions, appropriately oriented and scaled, are virtually identical to their counterparts in §4.2. One remaining feature is the presence of a zero in the $\hat{\phi}$-eigenfunction for $l = O(1)$; as l increases the zero shifts towards, and vanishes on reaching, z_1.

6. Results and discussion

Our study indicates that $O(\epsilon)$ two-dimensional periodic flows in the presence of $O(1)$ shear are unstable to longitudinal vortex form. Waves, however, do not drive the instability; they act as a catalyst and it is evident that wave distortion, caused by the back effect of the mean flow modification, affects that catalytic action. Least affected are short waves ($\alpha \to \infty$), so here the added complication of accounting for wave distortion is unjustified. But a different story is true for wavenumbers $\alpha \leqslant O(1)$, where wave distortion acts to diminish, and in some cases markedly suppress, catalytic action and thus the instability. Hence while the Craik–Leibovich type 2 instability does operate in arbitrarily strong inviscid shear flows, the timescale over which it operates will very likely depend upon the wavelength of the imposed waves: be they short the instability will grow exponentially until nonlinear effects are large enough to curb that growth; be they sufficiently long, an exponentially growing instability may not occur at all or, alternatively, the CL2 instability may endure long enough for longitudinal vortices to form, but then be suppressed owing to spanwise-periodic wave distortion.

Wave distortion also introduces eigenmodes of the standing-wave type: in the context of longitudinal vortices this means that such modes will align vorticity in the positive x-direction for half the cycle and the negative x-direction for the remainder. These modes occur on both sides of the (α_R, l_R)-curve, but they play little role on the short-wave side except in the nearest vicinity of the curve, where they alternately act to intensify and abate the longitudinal component of vorticity. On the long-wave side of the curve, however, such eigenmodes dominate and here the vortices may stand in space and alternate in sign. Of course this does not mean that vortex lines end and then begin in space at the instant the orientation of the longitudinal component of vorticity changes sign, but rather that the instantaneous vorticity vector has no longitudinal component at that instant. There is also the possibility, even likelihood, of individual rolls propagating spanwise with equal and opposite phase speeds.

As is evident from (2.8), the vorticity field $\hat{\Omega}(z)$ is determined primarily by $\bar{u}$ and $\hat{u}$, while from figures 5 and 9 we see that, as l increases, the turning point in $\hat{\Omega}(z)$ moves progressively closer to the boundary at which the mean velocity $\bar{u}$ relative to the wave is a minimum. Of course the turning point never reaches the boundary; rather, as $l \to \infty$ and σ_1 asymptotes to an upper bound, $\hat{u}$, and thus $\hat{\Omega}$, approach a limiting form. The vortex core is barely 20% of the z-domain in this limit compared with the whole z-domain for α and $l = O(1)$. Results without wave distortion are qualitatively the same. Thus, since $\hat{\Omega} = O(\sigma_1 l)$, we can say that higher growth rates give rise to vortices that are smaller and significantly more intense than lower growth rates. Further, because the vortices occur near the boundary at which $\bar{u}$ is minimum irrespective of wave amplitude, we can also say that shear and wave amplitude (each near its maximum) do not act in concert to focus longitudinal vorticity.

CL2 is a candidate instability for the formation of longitudinal, or more appropriately 'quasi-streamwise', vortices in turbulent boundary layers (Leibovich 1977; Craik 1985). Such vortices are most evident in the wall region (where the shear and turbulence intensity are greatest) and are closely linked to the regeneration of turbulence through events known as ejections and sweeps, collectively termed bursting. Specifically, transverse velocity components briefly peak to $O(\epsilon)$ values creating high levels of Reynolds stress as they do so. $\tilde{v}$ and $\tilde{w}$ then fade, but distinct axial velocity perturbations – streaks – remain and maintain a spanwise spacing almost

independent of scale. A most thorough account of events in the wall region is given by Robinson (1991).

Our longitudinal vortices of highest growth rate are also in the region of highest shear. But for their transverse velocity components to reach $O(\epsilon)$ requires $\delta = O(1)$, which invalidates (3.1) and very likely (2.13). Nonlinear counterparts to (2.13) and (3.1) can of course be constructed, but while we can reasonably expect nonlinearity to contain the instability we can be certain only that wave distortion will suppress it. Longitudinal vortices formed prior to suppression, however, may either continue to grow algebraically owing to the presence of newly formed oblique waves or undergo algebraic decay through viscous action. Interestingly, both scenarios give rise to an algebraic streamwise growth of the spanwise-varying part of $\tilde{u}$ (Phillips 1993), a curious parallel with the observed behaviour of streaks. Finally, viscosity is not necessary for the instability, but it will likely play a role at some (α, l) and of course allow the introduction of a second lengthscale. Only then can we view l in the context of streak spacing in a boundary layer and, to paraphrase McIntyre & Norton (1990), determine the ultimate fate of a viscous flow in which the initial vorticity is arbitrarily strong, subject to the instability.

We are grateful to Professor A.D.D. Craik for his interest and many helpful comments. The work was supported by the National Science Foundation grant CTS-9008477.

REFERENCES

ABRAMOWITZ, M. & STEGUN, I. A. 1965 *Handbook of Mathematical Functions*. Dover.

ANDREWS, D. G. & MCINTYRE, M. E. 1978 An exact theory of nonlinear waves on a Lagrangian-mean flow. *J. Fluid Mech.* **89**, 609–646.

BENNEY, D. J. 1964 Finite amplitude effects in unstable laminar boundary layers. *Phys. Fluids* **7**, 319–326.

BENNEY, D. J. & LIN, C. C. 1960 A non-linear theory for oscillations in parallel flow. *Phys. Fluids* **3**, 656–657.

CRAIK, A. D. D. 1970 A wave-interaction model for the generation of windrows *J. Fluid Mech.* **41**, 801–821.

CRAIK, A. D. D. 1977 The generation of Langmuir circulations by an instability mechanism, *J. Fluid Mech.* **81**, 209–223.

CRAIK, A. D. D. 1982*a* The generalized Lagrangian-mean equations and hydrodynamic stability. *J. Fluid Mech.* **125**, 27–35 referred to herein as *Ca*.

CRAIK, A. D. D. 1982*b* Wave-induced longitudinal-vortex instability in shear layers. *J. Fluid Mech.* **125**, 37–52 referred to herein as *Cb*.

CRAIK, A. D. D. 1985 *Wave Interactions and Fluid Flows*. Cambridge University Press.

HERBERT, T. & MORKOVIN, M. V. 1980 In *Laminar-Turbulent Transition* (ed R. Eppler & H. Fasel), pp. 47–72. Springer.

LEIBOVICH, S. 1977 Convective instability of stably stratified water in the ocean. *J. Fluid Mech.* **82**, 561–585.

LEIBOVICH, S. 1980 On wave-current interaction theories of Langmuir circulations. *J. Fluid Mech.* **99**, 715–724.

LEIBOVICH, S. 1983 The form and dynamics of Langmuir circulations, *Ann. Rev. Fluid Mech.* **15**, 391–427.

LEIBOVICH, S. & PAOLUCCI, S. 1981 The instability of the ocean to Langmuir circulations. *J. Fluid Mech.* **102**, 141–167.

LONGUET-HIGGINS, M. S. 1953 Mass transport in water waves. *Phil. Trans. R. Soc. Lond.* A **245**, 535–581.

MCINTYRE, M. E. 1988 A note on the divergence effect and the Lagrangian-mean surface elevation in periodic water waves. *J. Fluid Mech.* **189**, 235–242.

McIntyre, M. E. & Norton, W. A. 1990 Dissipative wave-mean interactions and the transport of vorticity or potential vorticity. *J. Fluid Mech.* **212**, 403–435.

Phillips, W. R. C. 1993 The genesis of longitudinal vortices in free and bounded shear layers. In *Eddy Structure Identification in Free Turbulent Shear Flows* (ed J. Bonnet & M. Glauser), pp. 35–41, Kluwer.

Robinson, S. K. 1991 The kinematics of turbulent boundary layer structure. *NASA TM* 103859.

Sarpkaya, T. & Henderson, D. O. 1984 Surface disturbances due to trailing vortices. *Naval Postgraduate School, Monterey, California, Rep.* NPS-69-84-004.